Skull Size and Biomechanics are Good Estimators of In Vivo Bite Force in Murid Rodents

Samuel Ginot, Anthony Herrel, Julien Claude, Lionel Hautier

Skull Size and Biomechanics are Good Estimators of *In Vivo* Bite Force in Murid Rodents

SAMUEL GINOT [1]* ANTHONY HERREL,[2] JULIEN CLAUDE,[1] AND LIONEL HAUTIER[1]

[1]Institut des Sciences de l'Evolution de Montpellier, Université de Montpellier, Montpellier, France

[2]Museum National d'Histoire Naturelle, Paris, France

ABSTRACT

Rodentia is a species-rich group with diversified modes of life and diets. Although rodent skull morphology has been the focus of a voluminous literature, the functional significance of its variations has yet to be explored in live animals. Myomorphous rodents, including murids, have been suggested to represent "high-performance generalists." We measured *in vivo* bite force in 14 species of wild and lab-reared murid rodents of various sizes and diets to investigate potential morphofunctional differences between them. We dissected their skulls and computed a biomechanical model to estimate bite force. We first tested if our model allowed good estimation of *in vivo* data. Then, using morphological, *in vivo* and estimated bite force data in a phylogenetic context, we aimed to find the drivers of bite force differences among species. Estimated and *in vivo* bite forces were strongly correlated, which indicates that (a) biomechanical models allow a good estimation of real performance, and that (b) size and muscular changes (increased mass, fiber length, and PCSA) are the main drivers of bite performance differences. Myomorphous rodents, therefore, may have evolved high bite force through a combination of changes in size and musculature, which gave them a great versatility in their ability to process food. We found mixed results at the intraspecific level, with only some species displaying a good fit between estimated and *in vivo* measurements. We suggest that limited variation in size and muscular organization, and increased behavioral variation might decrease the precision of bite force estimates within species. Anat Rec, 301:256–266, 2018. © 2018 Wiley Periodicals, Inc.

Key words: Muscle; adaptation; vertebrates; Muridae; bite force

Rodents are by far the most speciose group of mammals, while murids represent almost half of this specific diversity. Historically, variation in skull morphology has been used as a classification tool for rodents (Waterhouse, 1839, Brandt, 1855, Tullberg, 1899, Simpson, 1945; Wood, 1965; Hautier et al., 2015). Based on the relative importance of the distinct parts of the masseter muscle, as well as the positions of their origins and insertions on the cranium and the mandible, four combinations of skull morphologies are distinguished: sciuromorphy, hystricomorphy, myomorphy, and protrogomorphy (Supporting

Additional Supporting Information may be found in the online version of this article.

*Correspondence to: Samuel Ginot, Institut des Sciences de l'Evolution de Montpellier, Université de Montpellier, Batiment 22, Place Eugène Bataillon, Montpellier 34095, France. E-mail: samuel.ginot@umontpellier.fr

Received 16 March 2017; Revised 31 July 2017; Accepted 24 August 2017.

DOI 10.1002/ar.23711

Published online in Wiley Online Library (wileyonlinelibrary.com).

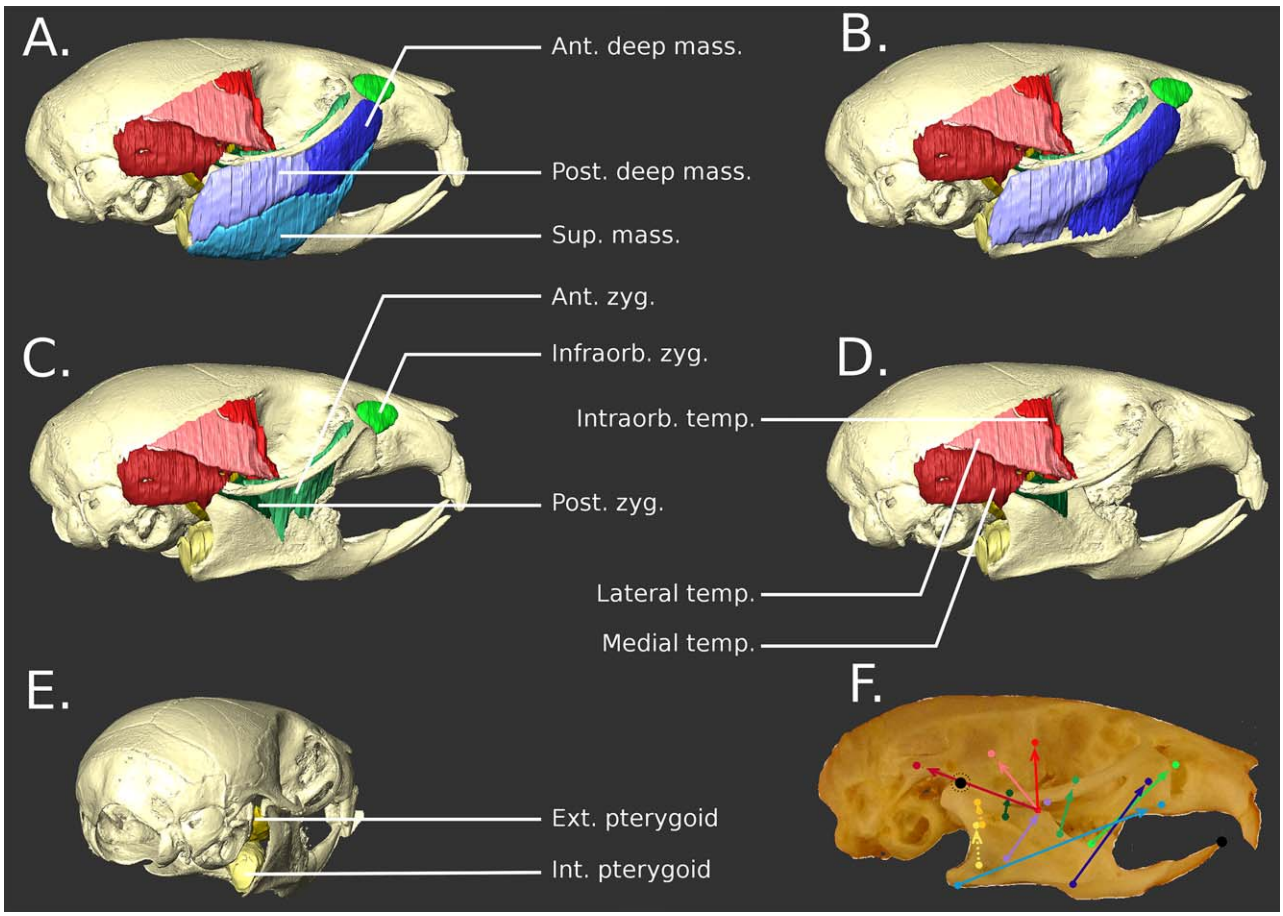

Fig. 1. (**A–E**) 3D rendering of the skull and muscles of *M. caroli*, obtained by iodine-enhanced CT scanning, as an example to illustrate Muridae skull morphology and musculature. (**F**) lateral view of the same skull, with arrows representing the lines of action of the muscles, and full circles representing theirs origins and insertions. The bigger black circles represent the point of application of the resistance force, and the point of rotation (dotted circle). Colors for all figures correspond to the different muscles. Sky blue: superficial masseter; dark blue: anterior deep masseter; pale blue: posterior deep masseter. Green: anterior zygomaticomandibularis; fluo green: Infraorbital zygomaticomandibularis; dark green: posterior zygomaticomandibularis. Red: intraorbital part of the medial temporalis; pale pink: lateral temporalis; dark red: medial temporalis. Yellow: internal pterygoid; golden: external pterygoid.

Information, Fig. 1). Among these morphotypes, the sciuromorphous and hystricomorphous rodents have been shown to specialize in gnawing and chewing, respectively. Myomorphous rodents, on the other hand, seem to encompass both gnawing and chewing, making them "high-performance generalists" (Cox et al. 2012; Maestri et al. 2016), overperforming both the sciuromorphous and hystricomorphous rodents in their respective specialties.

Myomorphs, murids especially, are the most diverse and widespread group among rodents. Their great adaptability, exemplified by several species that are spread across a wide latitudinal gradient and whose ecologies may range from feral to commensal within the same species (e.g. *Rattus tanezumi*, Aplin et al. 2011; *Mus musculus*, Berry and Jakobson 1975, Le Roux et al. 2002), might partly explain this diversity. This extraordinary lability is certainly related with their ability to exploit a wide array of food items (Navarrette and Castilla 1993, Le Roux et al. 2002, Corbalàn 2006, Samuels 2009, Maestri et al. 2016). Despite showing several dietary specializations (e.g. to carnivory, herbivory or insectivory; Samuels 2009), the murid skull morphology (Fig. 1) is often considered to be fairly stable (e.g., Rowe et al. 2011) in most species. This stable, but efficient, morphology was proposed to be related to an important functional versatility of their masticatory apparatus that enables most mice and rats to use various dietary resources (Cox et al. 2012). Still, the general morphological homogeneity should not be interpreted as a lack of adaptation or evolution. In fact, subtle but significant changes in skull morphology have been detected using geometric morphometrics (e.g. Siahsarvie et al. 2012, Michaux et al. 2007, Samuels 2009), dissections (e.g. Satoh and Iwaku 2006, 2008, Baverstock et al. 2013), iodine-enhanced CT scanning (e.g. Cox et al. 2011, 2012, Baverstock et al. 2013), and Finite Elements Analyses (FEA) methods (e.g. Cox et al. 2011, 2012). In most cases, these methods were used to better understand the relationship between phylogeny, phylogeography, function, and ecology. However, the functional consequences of the observed anatomical variation have remained poorly studied in live animals.

More specifically, how variation in the anatomy impacts ecologically relevant performance traits (bite force, speed, endurance, etc.) *in vivo* remains unknown. As making functional, ecological, and evolutionary inferences based on skull morphology and myology has been widely used in many fields from paleontology to ecology and development (e.g. Michaux et al. 2007, Samuels 2009, Satoh 1997, Satoh and Iwaku 2006, 2008), testing how these factors actually influence *in vivo* performance is necessary. Some studies have presented data on estimated bite force through muscular biomechanical models in rodents (e.g. Satoh 1997, Druzinsky 2010, Becerra et al. 2011). Yet, to our knowledge, only a handful of studies have so far validated morpho-functional estimations with *in vivo* measurements of bite force (Freeman and Lemen 2008a,b, Cox et al. 2012, Van Daele et al. 2009) Among them, only Van Daele et al. (2009) used a model based on the masticatory muscles for estimated bite force at an interspecific level (but see Nies and Ro 2004, Becerra et al. 2011 for intraspecific studies). In other vertebrate groups (*e.g.*, bats: Herrel et al. 2008a; shrews: Cornette et al. 2013, Young et al. 2007; lizards: Herrel et al. 1998a, 1998b), *in vivo* bite force was shown to be predictable by biomechanical estimates of the forces of the jaw adductor muscles (e.g. Herrel et al. 1998a, 1998b, 2008a). Bite force, whether *in vivo* or estimated, has been correlated with anatomy (size, shape, and myology) in various groups of animals (e.g. Verwaijen et al. 2002, Herrel et al. 2005, Santana et al. 2010). Ecologically, it also has been shown to play an important role in sexual competition (*e.g.*, Herrel et al. 2010), and feeding behavior and diet (e.g., Aguirre et al. 2003, Young et al. 2007, Herrel et al. 2008b, Santana and Dumont 2009). In light of these results, investigating bite force in myomorphous rodents is a great opportunity to better understand what functional advantage or structural constraints their unique skull morphology may hold.

Here, we aimed to test the predictive power of biomechanical models based on adductor musculature for bite force, and to explain any discrepancies between *in vivo* and estimated bite force, both at the intra- and interspecific levels. Doing so, we also tried to disentangle the effects of size, phylogeny, and muscular variation on bite force differences in our sample of species. Finally, we used our data to identify the modes of evolution of the muscular, bite force and size traits along the diversification of the rats and mice studied here which represent a small sample of the murid radiation.

MATERIALS AND METHODS

Specimens

In total, 75 rodents representing 14 different species were used in this study. Out of these, 68 were captured in the wild as part of the Ceropath and BiodivhealthSEA program fieldwork in Thailand in 2015 and 2016. Bite forces were measured directly after capture. Specimens were then euthanized and their heads were fixed in 70% ethanol before further treatment. Wild rodent specimens included in the study are neither on the CITES list, nor the Red List (IUCN). Animals were treated in accordance with the guidelines of the American Society of Mammalogists, and within the European Union legislation guidelines (Directive 86/609/EEC). Approval notices for trapping and investigation of rodents were provided by the Ethical Committee of Mahidol University, Bangkok, Thailand, number 0517.1116/661. The seven remaining specimens were acquired dead from animal facilities at the University of Montpellier (one *Mus mattheyi*, two *Mus minutoides*, two *Mus caroli* from the "KTK" strain and two *Mus pahari f*rom the "PAH" strain).

Bite Force Measurements

All *in vivo* bite force data were recorded at the incisors using a Kistler force transducer linked to a charge amplifier, similar to the set-up presented in Herrel et al. (1999) and Aguirre et al. (2002). After capture, we performed three consecutive trials for each animal. The maximal bite force recorded across the three trials was retained and used in subsequent analyses. We obtained *in vivo* bite force data for all wild individuals, and used the average species' values in our interspecific analyses. To broaden our interspecific data set, we added the lab specimens for which we used the averaged *in vivo* bite force obtained in their respective lab colonies.

Morphology

To test if biomechanical models could correctly estimate the *in vivo* data, we dissected the jaw musculature (Fig. 1) on one side for all specimens, and kept each muscle individually in 70% ethanol. We then blotted the muscle dry and weighted them with a 0.01 mg precision balance (Sartorius A 120 S). Next, muscles were transferred into a 30% nitric acid solution during 20 to 24 hours to separate their fibers. To stop the digestion the nitric acid solution was removed and replaced by a 50% glycerol solution. Finally, fibers were observed under a Wild Heerbrugg M3Z binocular microscope (ocular x10 Wild 445111, objective x1 Wild 411589) and 10–15 of them were selected randomly for each muscle and drawn using a camera lucida (Wild Heerbrugg TYP 308700). The drawings were scanned and the fiber lengths were then determined in ImageJ software. The muscular nomenclature used here follows that used in Baverstock et al. (2013), with the addition of a separate anterior and posterior deep masseter, and an orbital part of the medial temporal

Bite Model

The biomechanical model used to estimate bite force was similar to that described by Herrel et al. (1998a, 1998b), and relies on the computation of the static force equilibrium. As input for the model, the three-dimensional coordinates of the origins and the insertions and the physiological cross sectional areas of the jaw muscles are needed. Additionally, the three-dimensional coordinates of the point of application of the bite force and the center of rotation are needed (Fig.1F). These coordinates were determined by the mean of lateral and dorsal pictures of the skull with a 10-mm scale taken after the dissection (using a Pentax K200D reflex camera). For muscle with relatively broad areas of origin and insertion, the approximate centroid of the insertion area was used, based on knowledge from the dissections and literature data (e.g. Baverstock et al. 2013). All insertion and origin landmarks (Fig. 1F) were digitized using tpsDig2 software. Skull length was computed using the same pictures, in dorsal view by placing one

TABLE 1. Individual muscular data acquired for this study

Species	Specimen	Muscle mass (mg)			Muscle mass (mg) cont'd			Muscle mass (mg) cont'd			Muscle mass (mg) cont'd			Fiber length (mm)			Fiber length (mm) cont'd			Fiber length (mm) cont'd			Fiber length (mm) cont'd					
		Digas	DM.ant	DM.pos	M.sup	Pt.ext	Pt.int	Tp.I-O	Tp.lat	Tp.med	Zyg.ant	Zyg.I-O	Zyg.pos	Digas	DM.ant	DM.post	M.sup	Pt.ext	Pt.int	Tp.I-O	Tp.lat	Tp.med	Zyg.ant	Zyg.I-O	Zyg.post	In vivo bite force	Skull length (cm)
Berylmys berdmorei	7184	NA	179.6	101.4	118.6	124	62.5	28.5	24.4	81.7	16.5	63.2	8.8	5.84	5.84	5.21	5.56	2.43	3.6	3.56	4.73	4.57	4.25	4.59	2.3	21.26	5.41
B. berdmorei	7214	20.7	45.7	54.1	55	13.6	20	8.6	10.8	28.8	NA	21.8	3.9	3.37	4.01	3.45	4.37	2.31	3.12	3.63	3.59	3.5	NA	3.59	2.24	11.52	3.97
B. berdmorei	7215	24.6	70.9	52	63.1	20	20.8	18.2	NA	43.7	NA	36.8	15.9	3.11	3.26	3.29	3.61	3.34	2.92	2.95	NA	3.67	NA	3.46	2.45	15.4	4.58
Berylmys bowersi	7219	41.4	118	153.9	126.5	28.7	40.2	35.7	7.4	126.1	26.3	59.7	10.4	3.56	5.01	4.57	5	3.06	2.49	3.59	4.06	4.11	4.49	3.6	3.03	27.42	5.13
B. bowersi	7220	156.6	145.4	144.3	159.6	66	106.3	59.5	51.1	120.4	14.1	78.7	17.4	4.09	5.18	4.37	4.1	3.97	3.52	2.93	3.5	5.06	4.36	4.72	2.99	18.9	5.15
B. bowersi	7221	35.4	169.4	158.3	154	61	70.9	27.6	21.6	94.7	32.9	42.3	22.9	3.08	5.36	4.65	3.57	4.73	3.78	3.98	3.59	3.64	5.24	6.21	2.05	23.07	5.67
B. bowersi	7234	51.3	430.7	NA	191.3	NA	89.4	NA	19.8	217	19.2	80	10.5	5.93	5.93	NA	4.75	NA	3.59	NA	3.48	4.57	3.91	5.17	1.85	17.21	5.74
Berylmys sp.	7202	29.7	56.4	52.6	49	4.4	23.2	11.1	6.2	27.5	NA	24.9	8.8	3.82	3.52	3.33	3.71	2.05	3.07	2.96	2.95	4.41	NA	3.84	2.16	12.13	3.84
Maxomys surifer	7185	45.6	201.5	162.1	144.2	40.5	91.8	26.8	18.6	86.7	NA	87.8	21.1	3.83	4.04	3.78	3.6	3.53	3.01	3.56	3.33	3.38	NA	3.8	2.78	23.33	4.9
M. surifer	7186	24.4	97.5	97.5	91.7	29.2	41.2	18	11	49.9	14.3	25.7	7.1	3.55	NA	3.57	4.27	4.09	2.36	2.78	2.63	3.57	2.66	3.24	2.66	13.42	4.28
M. surifer	7187	22	94.9	94.9	85.9	20.1	24.5	NA	24.9	25.5	59.7	NA	10.8	3.87	5.77	4.91	4.82	3.36	3.33	NA	4.44	3.47	4.51	NA	2.83	18.08	4.51
M. surifer	7191	23.8	108.3	93.3	127.9	8.4	48.6	30.6	8.1	61.2	36.5	34	11.7	3.91	4.52	4.68	4.86	3.4	3.73	3.53	3.2	3.88	4.3	4.16	2.82	23.45	4.8
M. surifer	7192	29.5	117.4	103	108.7	29.8	25	17.9	12.4	51.9	16.4	52.9	3.9	4.43	6.13	6.05	5.25	3.65	4.99	3.28	3.8	3.83	3.08	5.24	2.34	26.05	4.86
M. surifer	7193	22.5	62.2	122.5	98	24.9	57.9	19.1	14.3	38.8	25.1	17.3	6.8	4.06	4.8	4.2	4.25	3	2.85	2.7	3.41	3.87	3.12	2.77	1.89	17.21	4.84
M. surifer	7194	36.1	122.6	111.7	103	50	769	34.3	12	60.5	16.4	42.2	17.1	3.96	5.74	5.05	4.67	4.19	3.83	3.58	4.02	3.98	4.36	3.78	2.58	22.69	4.93
Mus caroli	7195	2.2	8.8	7.9	8.6	1.2	4.3	2.2	1.6	4.9	1.5	1.5	1	2.28	3.45	3.35	3.57	2.81	2.89	2.77	3.07	3.13	3.13	3.38	1.86	1.87	2.05
M. caroli	7225	3.3	10.4	9.7	12	2.2	4.9	2.9	2.8	6.1	1	2.7	1.3	2.31	3.14	3.29	2.71	2.87	2.42	2.21	2.37	2.39	1.94	2.65	1.7	4.84	2.04
M. caroli	7236	4.5	9.1	7.3	7.8	2.4	3.5	1.5	1	7.2	NA	2.2	0.8	2.18	3.18	3.19	3.18	1.7	1.97	2.29	2.26	2.78	NA	2.45	1.94	2.77	1.86
M. caroli	7264	2	8.6	9.4	7.1	2.6	2.2	1.3	0.8	5.5	2.7	NA	0.8	2.57	3.66	3.05	2.99	2.85	3.02	2.46	2.62	3.1	3.21	NA	2.36	3.97	1.85
M. caroli	KTK24-13	5.2	31.7	NA	7.6	5	4.4	4.1	2.5	4	1.1	0.5	NA	4.13	4.05	NA	4.59	2.7	2.72	3.21	3.84	3.82	3.09	3.37	NA	9.69	2.28
M. caroli	KTK24-7	4.8	19.7	10.2	12.4	3	3	NA	4.2	4.9	1.9	1.8	0.9	3.85	4.7	4.41	4.61	3.84	3.15	NA	4.42	3.99	3.95	4.37	2.22	9.69	2.43
Mus cervicolor	7255	2.3	5.2	6.9	7.3	3	6.2	1.63	1.63	1.63	NA	2.1	2.1	2.67	3.38	3.59	3.48	3	2.72	2.33	2.46	2.85	NA	3.48	2.1	3.47	2.12
M. cervicolor	7258	2.2	4.1	4.6	6.3	1	1	1.2	NA	2.6	NA	1.1	1.1	2.57	3.55	2.92	2.49	2.53	2.35	3.04	NA	3.32	NA	3.77	1.73	3.09	2.07
M. cervicolor	7259	NA	5.5	6.7	7.6	3.6	5	1.6	1.4	4.4	1.3	1.1	0.2	2.69	2.69	3.49	2.82	3.69	2.03	2.73	2.91	2.75	2.49	2.72	1.93	3.88	2.13
M. cervicolor	7262	1.8	7.8	5.7	8.1	2.3	5.3	2.6	0.1	5.2	1.7	2.2	0.7	2.93	3.41	3.82	3.26	2.31	2.45	2.95	2.95	3.15	3.17	3.72	1.87	4.05	2.06
M. cervicolor	7263	1.6	6.4	3.9	6.3	0.9	3.4	0.1	0.1	3.7	3.2	NA	0.1	1.93	2.73	3.29	2.63	2.39	2.44	2.42	2.33	2.46	2.83	NA	1.88	3.88	1.94
M. cervicolor	7286	1.5	6	7.9	7.4	1.4	2.4	0.8	1.2	3.9	1.2	NA	1.2	2.9	3.22	3.43	2.84	3.08	2.78	3.04	3.55	3.59	2.96	NA	2.5	3.3	2.13
M. cervicolor	7304	3.2	7.3	6.4	9.2	5.4	6	2.1	0.1	9	2.1	2.1	0.1	2.39	3.26	3.55	3.08	3.55	3.07	2.47	2.79	2.59	2.67	2.87	1.52	2.89	2.1
M. cervicolor	7313	2.1	6.3	6.7	9.2	1.6	5.6	1.6	1.1	3.8	1.2	0.9	0.7	2.37	2.82	3.23	3.11	2.37	2.4	3.08	2.06	2.79	2.46	3.23	1.77	3.59	1.95
M. cervicolor	7314	6.6	12.8	10	15.2	4.4	10.3	4.2	2.4	9.3	1.6	3.9	0.9	3.1	2.9	3	2.98	2.84	3.02	2.45	3.14	2.9	2.59	3.14	2.02	4.81	2.06
M. cervicolor	7315	3.9	7.4	9.5	11.5	1.8	4.7	2.8	2.3	6.5	NA	3.2	0.6	2.6	2.98	3.04	2.87	2.33	2.35	2.84	3.18	3.38	NA	2.44	1.87	5.4	2.02
Mus cookii	7210	4.8	8.3	13.1	16	6.6	9.3	3.2	2.2	6.9	NA	5.4	1.8	2.52	2.68	2.99	2.76	2.77	2.47	2.45	3.34	3.13	NA	2.6	2.15	6.1	2.12
M. cookii	7238	2.8	9.2	12.5	13.6	3.6	3.9	3.4	1.2	7.2	3.2	1.7	1.5	3.33	3.58	3.87	3.53	2.23	2.96	2.78	3.11	3.25	2.97	3.54	1.85	4.46	2.17
M. cookii	7239	3.3	9.6	7.3	9.3	2.7	7.4	1.5	1	5	NA	2.2	2.2	2.75	3.18	3.3	3.33	2.58	2.83	3.09	2.71	3.31	NA	3.26	1.67	4.84	2.4
M. cookii	7243	NA	8.1	14.3	19.6	5.8	11.5	5.4	1.5	9.6	1.9	2.9	1.1	3.83	3.83	3.56	3.17	3.07	2.68	2.68	2.99	3.14	2.97	2.96	2.41	4.7	2.42
Mus fragilicauda	7254	3.9	5.6	16.6	15.3	4.1	4	2.3	NA	12.7	NA	5.6	0.8	3.4	3.03	3.32	3.22	2.15	2.52	3.22	NA	3.19	NA	3.14	2.58	4.52	2.29
M. fragilicauda	7261	1.2	3.7	5.5	6.4	0.1	1.9	0.2	1.4	2.6	NA	1.5	0.6	2.67	2.57	3.43	3.34	2.76	2.52	2.02	2.32	2.74	NA	2.83	1.58	4.26	2.1
Mus mattheyi	mattheyi1	NA	1.6	3.6	2.4	0.6	1.5	NA	0.7	1.9	0.8	0.8	0.8	2.74	2.74	3.52	3.45	2.6	2.26	NA	2.84	2.77	2.51	2.88	1.81	2.48	1.88
Mus minutoides	minut1	1.1	3	3.4	3.3	2	3	NA	2.4	2.4	1.6	1.6	1.6	3.07	3.24	3.64	3.58	1.91	1.65	NA	1.64	1.9	2.83	3.7	1.25	3.52	2.12
M. minutoides	minut2	1.4	3.6	4.4	5.2	1.5	3.1	NA	0.1	4	1.3	1.3	0.1	2.7	2.72	2.97	2.79	2.81	2.23	NA	2.8	2.63	2.39	2.68	1.87	3.52	2
Mus pahari	7226	5.2	9.1	16.7	16.1	4	13.5	7.8	3.7	5.4	NA	4.1	0.8	2.77	3.18	3.39	4.03	3.01	3.37	2.67	2.7	2.89	NA	2.77	1.7	7.58	2.47
M. pahari	7235	4	11.4	12	13.5	0.8	3.5	1.2	0.7	7	NA	5.6	0.7	2.93	3.2	3.23	3.37	2.07	2.86	2.37	2.69	3.29	NA	2.59	1.93	5.54	2.55
M. pahari	PAH54-7	NA	17.9	17.9	27.3	5.6	1.5	4.6	7.1	6.1	2.7	7.8	2.3	4.87	4.87	3.72	4.5	3.29	3.74	3.6	3.79	3.74	3.84	3.58	3.07	10.22	3.09
M. pahari	PAH54-9	4	18.1	17	27.2	3.7	11.3	5.5	5.2	8	2.3	6.9	1.7	3.83	4.22	3.56	4.29	3.81	3.37	3.98	4.04	3.64	3.51	4.03	3.3	10.22	2.96
Niviventer fulvescens	7198	25.9	92	89.1	98.4	22	33	21.6	4.3	37.2	10	30	7.5	3.53	4.18	3.88	3.73	2.54	2.24	3.02	3.68	3.07	3.75	3.86	2.39	20.94	4.11
N. fulvescens	7200	22.2	49.8	76.4	59	9.6	12.7	9.8	12	19.7	7	19.5	5.6	3.57	3.18	3.61	4.26	3.13	3.07	2.66	2.56	3.1	3.1	3.44	2.24	16.63	3.84
N. fulvescens	7227	2.7	20.7	14.6	17.4	0.5	12.1	6.2	0.7	4.1	1.6	0.8	0.2	2.76	3.24	2.92	3.13	2.63	1.98	2.4	3.16	2.84	3.41	2.35	2.17	7.23	2.98
N. fulvescens	7240	31	62	83.3	82.1	34.4	53.4	25.1	9.6	37.3	5.8	28.7	8.8	4.47	3.21	2.99	3.62	2.33	2.24	3.19	3.53	3.88	2.55	3.58	3.01	14.61	4.25
N. fulvescens	7244	15.9	96.4	67.5	67.1	26.3	10.8	8.7	9.9	38	NA	34.8	4.9	3.05	4.33	3.97	3.95	3.06	2.84	2.92	3.56	3.8	NA	4.77	2.57	17.38	4.09
N. fulvescens	7245	25.5	71	63.5	84.5	18.7	45.7	20.2	12.6	46.6	9.9	37.4	3.3	2.9	3.33	3.01	3.71	1.99	2.65	2.86	3.22	3.13	2.81	3.34	2.27	17.06	4.44
N. fulvescens	7246	22.5	84.2	62.4	91	17	34.9	27.9	16.1	39.5	29.15	29.15	9.8	2.82	4.14	3.85	3.86	3.43	2.64	2.41	3.14	2.97	2.74	3.41	2.61	12.8	3.83
N. fulvescens	7248	NA	59.4	73.9	69.7	7.5	38.1	10.2	14.7	38.4	17	18.5	8.2	3.59	3.59	3.46	3.1	2.17	2.75	2.57	2.56	3.49	3.21	3.03	1.95	16.6	3.96
Rattus andamanensis	7216	62.6	245	132.7	190.5	73.6	117.5	72.1	14.2	183.6	40.2	61.1	15.2	4.24	4.41	5.86	4.54	3.55	2.93	3.43	6.03	4.27	3.73	4.51	2.95	26.98	5.44
Rattus exulans	7267	NA	17	24.5	19.4	11.7	5.3	5.6	3.1	13.5	6.8	5.7	2.4	3.56	3.56	2.74	3.79	2.89	2.36	2.43	3.24	2.99	3.74	3.61	1.71	7.38	2.9
R. exulans	7288	6.5	23.3	23.7	17.3	4.6	8.4	5.2	4.1	13.6	4.2	5.5	0.8	3.13	2.79	3.07	2.79	2.22	1.9	2.43	2.77	2.8	2.8	3.07	1.71	4.61	2.99
R. exulans	7291	7.7	27.8	27.6	30.2	NA	66.5	NA	2	26	1	10.7	1.3	3.89	3.94	3.8	4.47	NA	2.56	NA	3.5	3.76	2.95	5.01	1.55	6.68	3
R. exulans	7292	13.2	27.3	10.3	33.4	4.5	4.6	NA	6.1	23.1	NA	13.5	NA	2.24	2.66	2.8	2.87	2.15	1.83	NA	3.05	3.54	NA	2.7	NA	8.05	2.98
R. exulans	7296	6.7	21.7	19.7	22.6	4.5	7.3	7.6	3.2	12.9	13.3	NA	1.4	2.82	3.87	4.01	4.54	2.1	2.54	3.48	4	3.59	3.4	NA	1.94	7.82	3.09
R. exulans	7298	4.8	25.9	25.9	23.4	7.7	12.4	7.1	5.8	15.5	4.1	7.3	2.6	2.68	3.99	3.4	3.9	2.62	2.51	2.92	3.29	3.95	3.41	3.39	2.44	8.9	3.06
R. exulans	7306	6.5	20.2	18.4	19.3	5	7.8	6.8	3.3	12.9	3.5	5.3	2.3	3.61	3.62	3.3	3.53	2.8	2.19	2.82	3.43	3.63	3.31	4.23	2.4	6.27	2.88
R. exulans	7311	11.5	29.5	28.4	38.4	5.6	14.2	5	8.6	24.7	NA	14.5	1.1	2.77	4.18	3.71	4.2	1.96	2.07	2.76	4.08	3.55	NA	3.57	1.83	8.78	3.13
Rattus tanezumi	7201	14.8	37.4	47.6	39.3	16.1	25.4	13.6	8.5	26.1	8.8	11.3	NA	3.26	3.33	3.29	3.82	2.13	2.32	2.2	3.03	3.37	3.24	3.17	NA	15.6	3.27
R. tanezumi	7206	19.9	62.7	59.2	75.4	11.9	26.8	5.6	8.6	39.8	7.1	21.5	3	3.11	3.51	3.09	3.92	2.96	2.32	2.46	3.45	3.4	3.27	3.84	2.47	23.63	3.67
R. tanezumi	7208	16.1	49.7	47.3	52.2	16	27.9	15.3	9.5	27.6	9.6	15.6	3.8	3.77	4.69	4.84	5.45	4.06	3.77	3.54	3.86	4.55	3.91	5.46	2.01	22.02	4.06
R. tanezumi	7209	10.8	55.5	39.4	63	7.2	22	17	4.7	34.8	NA	12.2	2.5	3.36	3.44	3.35	3.49	2.73	2.12	2.97	3.16	3.87	NA	3.44	1.72	17.06	3.43
R. tanezumi	7217	23.8	75.3	58.5	89.6	14.1	37.1	13.1	9.6	45.1	15.3	13.5	4.6	3.87	4.5	5	5	4.3	3.4	3.25	3.99	4.21	4.61	5.67	2.13	20.56	3.62
R. tanezumi	7257	21	76.2	82.9	93	14.6	27.6	30.9	15.6	39.2	46.1	18.8	4.4	3.25	4.36	3.5	4.47	2.71	2.36	3.08	3.44	2.82	4.3	4.08	2.55	28.38	3.98
R. tanezumi	7270	26.3	123.5	90.8	98.2	10.4	18	19.9	13.5	80.4	17.5	19.7	4.4	3.38	4.72	4.76	4.97	3.21	2.65	2.71	4.11	4.06	3.53	5.13	2.32	22.2	4.27
R. tanezumi	7273	55.9	166	130.2	156.7	26.9	25.8	66.6	40.1	68.2	32.2	30.1	12.4	4.07	5.25	3.05	5.92	2.16	3.85	3.75	4.34	3.01	4.1	4.97	2.49	28	4.74
R. tanezumi	7284	25.6	82.3	126.5	96.1	23.1	68	26.1	14.3	73.5	26	20.2	12	4.18	4.73	4.59	4.63	3.14	3.04	3.82	3.2	4.39	4.16	3.56	2.47	26.19	4.06
R. tanezumi	7302	35.4	77.3	139.6	126.7	22.7	72.4	29.1	22	106.9	17.3	31.6	13.9	4.47	5.64	4.9	5.42	2.96	3.1	4.03	4.86	5.91	4.36	4.27	3.03	15.9	4.26
R. tanezumi	7317	45.8	125.4	207.5	133	8.5	22.8	30.6	16.9	90.5	NA	70.5	11.4	4.19	4.19	4.23	4.36	2.53	2.16	3.2	4.04	4.6	NA	4.51	2.84	23.45	4.88
R. tanezumi	7319	8.9	29.1	18.5	22.3	4.1	17	3.3	4.2	16.8	NA	23.4	7	3.12	2.84	2.94	2.92	2.7	2.27	2.31	3.15	3.21	NA	2.74	1.26	11.93	3.44
R. tanezumi	7320	49.2	98	140.5	145.5	9.1	47	28	37.6	130.5	NA	67.8	22.1	4.71	5.38	7.12	6.37	2.96	2.84	3.17	4.88	4.46	NA	5	3.66	22.55	4.61

Abbreviations for muscle names are as follows: Digas = digastric; DM.ant = anterior deep masseter; DM.pos = posterior deep masseter; M.sup = superficial masseter; Pt.ext = external pterygoid; Pt.int = internal pterygoid; Tp.I-O = intraorbital part of the temporalis; Tp.lat = lateral temporalis; Tp.med = medial temporalis; Zyg.ant = anterior zygomaticomandibularis; Zyg.I-O = infraorbital zygomaticomandibularis; Zyg.pos = posterior zygomaticomandibularis.

landmark at the most anterior tip of the nasal bones and a second at the most posterior point of the occiput, and calculating the distance between them. Skull length was used as the size estimator throughout the analyses.

Physiological cross sectional areas (PCSA) were calculated based on the mass of the muscles, a density of 1.06 g cm^{-3} (Mendez and Keys, 1960), and the average fiber length for each muscle.

$$PCSA = \frac{\text{Muscle mass}}{1.06 \times \text{fiber length}}$$

As complex pennate muscles were separated into their component parts, no additional correction for pennation was considered. To calculate muscle forces, cross sectional areas were multiplied by a conservative muscle stress estimate of 30 $N.cm^{-1}$ (Herzog 1994), and by the cosine of the angle (Φ) of the muscle vector relative to the reaction force on the teeth (set vertical).

$$\text{Muscle force} = PCSA \times 30 \times \cos(\Phi)$$

Muscular data used are presented in Table 1.

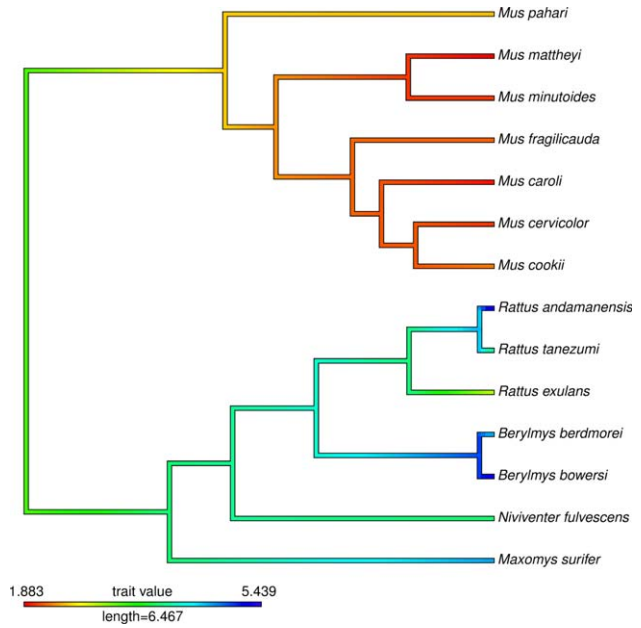

Fig. 2. Phylogenetic tree used in this study (extracted and modified from Fabre et al., 2013), with skull size mapped onto it (blue = larger; red = smaller) using the contMap function of package "phytools" in R.

Statistical Analyses

All analyses were run in R software (R Core Team 2016) and all data were natural log-transformed before analyses. For interspecific level analyses, we computed the species means for bite force and muscular variables. When looking at the influence of muscular variables on bite force, we grouped muscle of the same muscular group together rather than using separate values (to reduce the number of explanatory variables and allow the use of specimens with missing values). Thus, we ran the analyses with five muscle groups: superficial masseter, deep masseter, temporalis, pterygoid, and zygomaticomandibularis. We used the same muscular variables, and calculated and *in vivo* bite force, to test their scaling with size. Finally we ran the same scaling analyses using independent contrasts of size, muscular variable, and estimated and in vivo bite force.

To test the validity of our bite force estimates we correlated individual values to their corresponding *in vivo* observations, both at the interspecific and intraspecific levels (in species for which eight or more specimens had both values available). A redundancy analysis (RDA) was used to visualize which muscular variables were the main drivers of bite force variation. For this analysis only, we used raw (rather than log transformed) values centered on their means and scaled to unity variance, since our variables had different units. Muscular attributes (including fiber length, muscle mass, and muscle PCSA) were our response variables, while size, *in vivo* and estimated bite force were the explanatory variables. This RDA also allowed us to test which muscular traits were at the root of the discrepancies between *in vivo* and estimated bite force.

To test the potential effect of phylogeny and size on bite force, we pruned a tree from the one published by Fabre et al. (2013) with divergence time estimates. *Mus mattheyi* and *Mus fragilicauda* were missing from the

TABLE 2. Scaling of muscular traits (mass and fiber length) and bite forces against skull size at the interspecific level

	Slope	Estimate	SE	*t* value	*P* value
Mass DM	**3.373**	0.373	0.101	3.697	<0.001
Mass M.sup	3.191	0.191	0.1099	1.737	0.0866
Mass Ptery	3.148	0.148	0.1953	0.76	0.45
Mass Temp	**3.301**	0.3009	0.1304	2.308	<0.05
Mass Zyg	**3.602**	0.6016	0.1216	4.949	<0.001
Fiber DM	**0.365**	−0.635	0.0635	−9.995	<0.001
Fiber M.sup	**0.4247**	−0.5753	0.0523	−10.99	<0.001
Fiber Ptery	**0.1989**	−0.8011	0.0671	−11.94	<0.001
Fiber Temp	**0.3936**	−0.6064	0.0622	−9.742	<0.001
Fiber Zyg	**0.5266**	−0.4734	0.0943	−5.021	<0.001
In vivo bite force	2.013	0.0126	0.0959	0.132	0.895
Estimated bite force	**2.843**	0.843	0.0967	8.713	<0.001

Values in bold differ significantly from their expected slopes (1 for fiber length, 3 for muscle mass, and 2 for bite force). Abbreviations for the groups of muscles are as follows: DM = deep masseter; M.sup = superficial masseter; Ptery = pterygoids; Temp = temporalis; Zyg = zygomaticomandibularis.

TABLE 3. Scaling of the independent contrasts of muscular traits and bite forces against the independent contrasts of size

	Slope	Estimate	SE	*t* value	*p* value
Mass DM (IC)	3.197	0.197	0.276	0.715	0.49
Mass M.sup (IC)	3.126	0.126	0.291	0.435	0.672
Mass Ptery (IC)	3.607	0.607	0.326	1.86	0.09
Mass Temp (IC)	**3.743**	0.743	0.319	2.332	0.04
Mass Zyg (IC)	3.309	0.309	0.162	1.906	0.083
Fiber DM (IC)	**0.521**	−0.479	0.052	−9.196	<0.0001
Fiber M.sup (IC)	**0.063**	−0.937	0.087	−10.72	<0.0001
Fiber Ptery (IC)	**0.442**	−0.558	0.079	−7.084	<0.0001
Fiber Temp (IC)	**0.628**	−0.372	0.138	−2.686	0.021
Fiber Zyg (IC)	0.872	−0.128	0.253	−0.505	0.623
In vivo bite force (IC)	1.505	−0.495	0.24	−2.06	0.064
Estimated bite force (IC)	**2.766**	0.766	0.247	3.101	0.01

Expected slopes and abbreviations are the same as in Table 2.

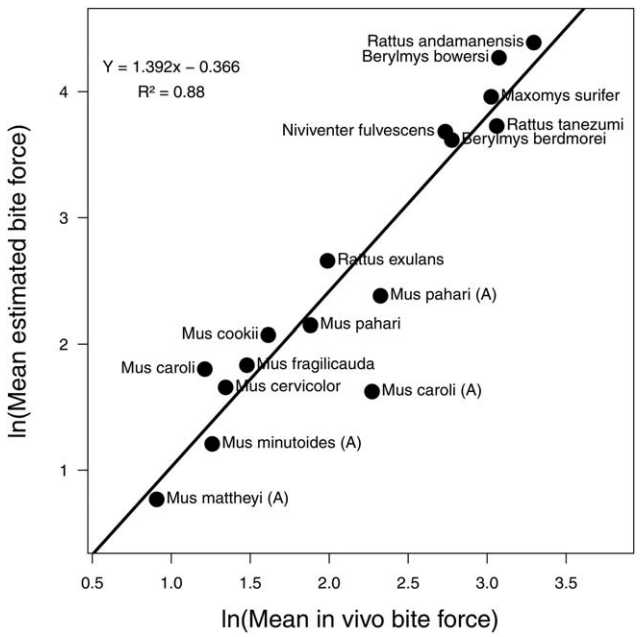

Fig. 3. Plot showing the linear relationship between log transformed *in vivo* and estimated bite force at the interspecific level. Each point represents the average value for one species. (A) denotes lab-reared populations.

tree, and were added using divergence times from Veyrunes et al. (2005) and Suzuki et al. (2004) (Fig. 2).

As size is usually the main variable driving differences in bite force and morphology, most studies have used residuals from linear regression of the trait of interest against size to filter out the effect of size. Because they are not orthogonal from the regression line, ordinary residuals from linear regressions can still covary with size as a technical artefact. Therefore, instead of linear regressions, we computed orthogonal regression of estimated bite force against size, and of *in vivo* bite force against size and used the minor axis as a size corrected variable. We were then able to calculate independent contrasts (IC) for our size independent variables (i.e., the aforementioned minor axis), to assess their correlations when accounting for phylogenetic nonindependence (Felsenstein 1985).

Using orthogonal regression, we computed the major and minor axis of covariation of muscular data (fiber length, mass and PCSA) with size. We also calculated the IC for the size-independent axes of covariation for PCSA, muscle mass and fiber lengths, and tested their correlation with *in vivo* bite force and estimated bite force. We used the fitContinuous function from the R package Geiger (Harmon et al. 2008), to check for phylogenetically driven variation in our sample, and to compare between different models of the evolution of bite force, size, and muscular variables. We fit Brownian Motion (BM), Ornstein-Ulhenbeck (OU), lambda, Early Burst (EB) and White Noise (WN) models, and used AIC to assess which of them best described the evolution of bite force. We used the same function to test for models of size and muscle evolution along the diversification of mice and rats.

As bite force estimations are sometimes imprecise at the intraspecific level, we also tested this in our sample. We performed some analyses at the intraspecific level in four species for which we had eight or more representatives. Again, we correlated *in vivo* bite force and estimated bite force as well as their correlation to skull size. As with interspecific analysis, we computed orthogonal regressions to check if size-independent *in vivo* bite force and estimated bite force would still be significantly linked.

RESULTS

Scaling of Variables to Size

Most muscle groups had significant positive allometries for their mass (with the exception of the superficial masseter and pterygoid), with slopes much higher than the expected value of 3 predicted by geometric similarity models. On the other hand, fiber lengths showed negative allometries for all muscle groups with slopes significantly smaller than the expected value of 1. For bite force, allometries differed, with *in vivo* bite force being isometric, while estimated bite force showed significant positive allometry (Table 2). Different results were found using independent contrasts (Table 3), with muscle mass scaling with the expected slope of 3, excepted for the temporalis which shows significantly positive allometry. As with the nonphylogenetic analyses, fiber lengths scaled with size with significantly smaller than expected slopes, except for the zygomaticomandibularis. Finally, *in vivo* bite force did not have a slope significantly different from isometry, but estimated bite force had significantly positive allometry, as was found with the nonphylogenetic analyses.

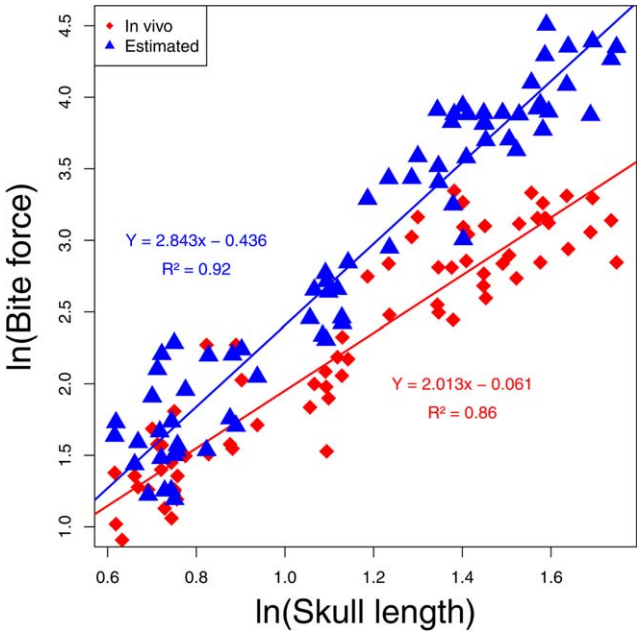

Fig. 4. Plot showing the difference in the scaling of log transformed *in vivo* bite force and estimated bite force against size. Both slopes are significantly different with slope∼2 for *in vivo* bite force (red diamonds) versus slope∼2.8 for estimated bite force (blue triangles).

Correlation Between Bite Force Values

We computed biomechanical estimates of bite force and compared them to our *in vivo* data. At the interspecific level, the log transformed values showed a very significant correlation ($r^2 = 0.88$, $P < 0.001$) (Fig. 3). Lab-reared populations of *M. pahari* (PAH) and *M. caroli* (KTK) deviated from this relationship, with much higher *in vivo* than estimated bite force. The slope of the linear regression between *in vivo* and estimated bite force was >1 (slope = 1.4, $t = 3.08$, $P < 0.01$), meaning that estimates diverge slightly but significantly from measured bite force (Fig. 4). Orthogonal regressions revealed that size explained most of the variance of *in vivo* bite force and estimated bite force (89% and 88%, respectively). Residuals (i.e., minor axis) from these regressions were still strongly related ($r^2 = 0.67$, $P < 0.001$), which shows that the good fit of estimated bite force is not only explained by size.

Redundancy analysis (RDA) (Fig. 5)

The RDA was performed on muscular variables constrained by size, estimated, and *in vivo* bite forces. This analysis allowed us to pinpoint the muscular attributes that correlate with each of these three constraining variables (size, *in vivo* bite force, and estimated bite force). It showed that 87% of the variance in muscular attributes was "redundant" with (i.e., explained by) the constraining variables, while 13% remained, independent of the constrained axes. As expected, we found that the first constrained axis is mainly linked to size, and that all muscular variables, and bite forces, are correlated to it (Fig. 5A). We also showed that *in vivo* bite force and estimated bite force are divergent along the second constrained axis. Therefore, the variables that explain this

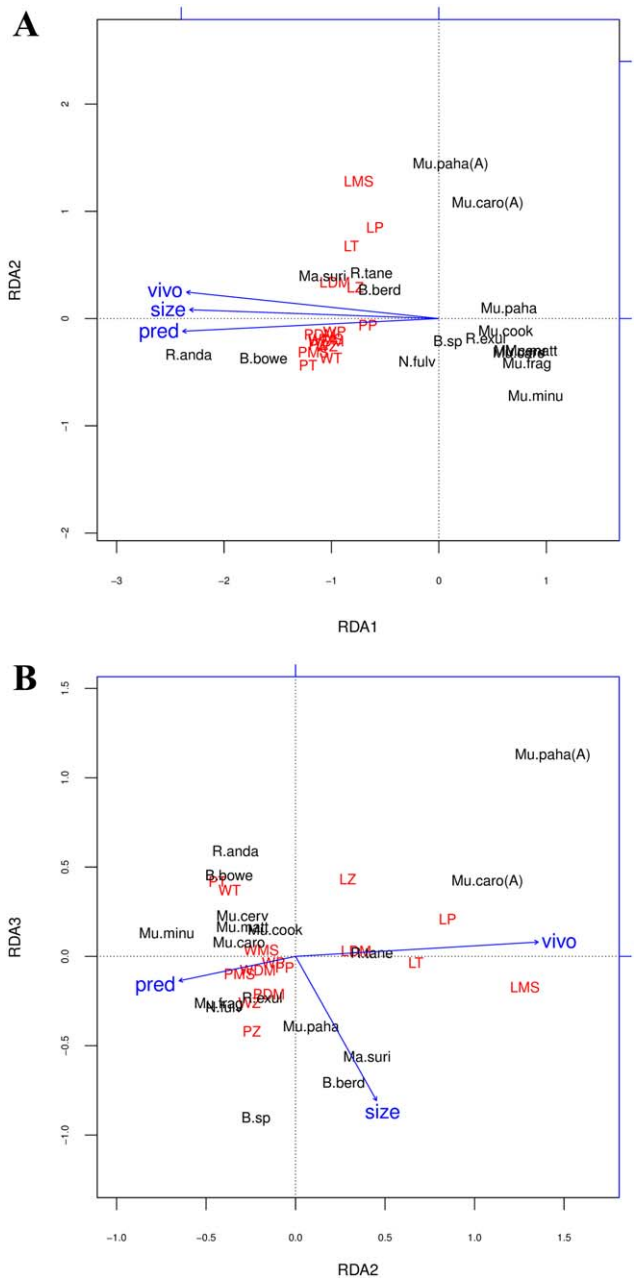

Fig. 5. Plot of the RDA run on muscular variables, constrained by bite forces and size. (**A**) Constrained axes 1 and 2. (**B**) Constrained axes 2 and 3. Species names are abbreviated. B.berd: *Berylmys berdmorei*; B.bowe: *Berylmys bowersi*; M.suri: *Maxomys surifer*; M.caro: *Mus caroli*; M.cerv: *Mus cervicolor;* M.cook: *Mus cookii;* M.frag: *Mus fragilicauda*; M.matt: *Mus mattheyi*; M.minu: *Mus minutoides*; M.paha: *Mus pahari*; N.fulv: *Niviventer fulvescens*; R.anda: *Rattus andamanensis*; R.exul: *Rattus exulans*; R.tane: *Rattus tanezumi*; M.caro(A): lab-reared *Mus caroli;* M.paha(A): lab-reared *Mus pahari*. Variables abbreviations as follow, pred: estimated bite force; vivo: in vivo bite force; size: skull length; LDM, LMS, LP, LT, LZ: mean muscular fiber lengths for the deep masseter, superficial masseter, pterygoid, temporal and zygomaticomandibularis muscular groups, respectively; WDM, WMS, WP, WT, WZ: mean muscle mass for the same muscular groups; PDM, PMS, PP, PT, PZ: mean PCSA for the same muscular groups.

divergence should scale along this axis. Interestingly, it appeared that the ordination of muscular attributes along axis RDA2 mainly separates fiber lengths, correlated with *in vivo* bite force, from muscular masses and PCSAs, which correlated with estimated bite force (Fig. 5B).

Effect of the Phylogeny on Bite Force, Size, and Muscular Variation

Independent contrasts of both *in vivo* and estimated bite forces were very tightly correlated to the independent contrasts of size ($r^2 = 0.68$ and $r^2 = 0.89$, respectively, with $P < 0.001$) at the interspecific level. Moreover, the IC of size-independent *in vivo* bite force and estimated bite force (obtained by orthogonal regression) were strongly correlated ($r^2 = 0.87$, $P < 0.0001$). As expected, the IC of PCSA, muscular mass and fiber length also showed robust correlations (length vs mass $r^2 = 0.74$, mass vs PCSA $r^2 = 0.96$, PCSA vs length $r^2 = 0.78$ with all $P < 0.0001$). However, we found no correlation between the IC of either *in vivo* bite force or estimated bite force and PCSA, muscle mass, or fiber length (all $P > 0.3$).

To complement these analyses and better understand how phylogeny influenced musculature and bite force, we tested models of evolution for size-independent *in vivo* bite force, estimated bite force, and size. For both *in vivo* bite force and estimated bite force, white noise model showed the best results (i.e., lowest AIC), while for size lambda model was selected, showing significant phylogenetic signal (lambda = 0.71, $P < 0.01$). Similar to bite force, size independent variation in PCSA, fiber length, and muscle mass were best described by the white noise model.

Variation in Muscular Attributes and Bite Force

Using size-independent muscle masses, PCSA, and fiber lengths, we found that the size independent axes of muscular covariation was not significantly correlated with the size independent bite force axes, suggesting that muscular changes did not relate significantly to bite force changes (both *in vivo* and estimated). Similar results were obtained with the IC of PCSA, fiber lengths, and muscle mass, compared to the IC of *in vivo* bite force and estimated bite force. In any case, we found that only a rather small part of muscular variation was independent of size, with about 13% for PCSA and 12% for muscle mass. Fiber length, however, showed 20% of size-independent variation.

Intraspecific Level Analyses

Four species in our dataset had eight or more specimens with associated *in vivo* bite force, dissections and therefore estimated bite force data: *Rattus tanezumi* (N = 13), *Mus cervicolor* (N = 10), *Rattus exulans* (N = 8), and *Niviventer fulvescens* (N = 8). For *R. tanezumi* and *M. cervicolor*, a significant correlation between *in vivo* and estimated bite force was found (respectively $r^2 = 0.61$, 0.66 and $P < 0.05$). *N. fulvescens* showed marginally significant correlation ($r^2 = 0.7$, $P = 0.052$); however, this was mainly driven by one juvenile outlier, whose removal from the analysis produced a nonsignificant correlation ($P > 0.8$). No correlation was found in *R. exulans*.

In *R. tanezumi*, both *in vivo* bite force and estimated bite force were correlated with skull size ($r^2 = 0.57$ and 0.83, with $P < 0.05$ and $P < 0.001$, respectively). When looking at size-independent (i.e., after orthogonal regressions against size) *in vivo* bite force and estimated bite force, the correlation remained significant ($r^2 = 0.59$, $P < 0.05$), suggesting that musculature differences at the individual level drive bite force differences.

In *M. cervicolor*, *in vivo* bite force and estimated bite force were not significantly correlated with skull size, and the correlation between them actually improved when using their size-independent values (from $r^2 = 0.66$, $P < 0.05$ to $r^2 = 0.95$, $P < 0.0001$). It is worth noting that skull size variance was very small in our sample of *M. cervicolor*.

In *R. exulans*, neither estimated bite force nor *in vivo* bite force were significantly linked to size. However, size-independent estimated bite force and *in vivo* bite force were correlated ($r^2 = 0.79$, $P < 0.02$). Similarly to *M. cervicolor*, *R. exulans* had a very small variance in skull size.

DISCUSSION

The predictive power of our biomechanical model is good (Fig. 3) with size being, as expected, the main explanatory variable for the variation in both estimated and *in vivo* bite force. Divergence between estimates and *in vivo* measurements are clearly shown by the differences in their scaling with size (estimated bite force has positive allometry, while *in vivo* bite force is isometric Fig. 4 and Table 2). RDA showed that this divergence is mainly due to differences in which muscular attributes are correlated with bite force (Fig. 5). *In vivo* bite force is more dependent on fiber length variation while estimated bite force is more dependent on muscle mass variation. This result is coherent with their differences in allometry, as muscle mass (linked to estimated bite force) shows positive allometry while fiber lengths (linked to *in vivo* bite force) show negative allometry. It therefore appears that higher values of estimated bite force are probably linked to the higher estimated muscular mass (Fig. 5). The RDA also showed that all muscular groups were indifferently involved in the variation of bite forces. The differences between estimated and *in vivo* bite force may be explained by imperfections in the biomechanical model, due to errors in dissections or fiber measurements for example, or by the fact that in vivo bite force is influenced by many biological factors, as well as by the settings of the force transducer. In any case, the very good correspondence between *in vivo* and estimated bite force shows that using dissections to estimate bite force can yield results very close to reality. Therefore, using biomechanical models for rodents when *in vivo* bite force data are unavailable is entirely justified.

At the intraspecific level, it appears that the biomechanical model has good results only in some cases. The lack of accuracy may be due to small sample size with animals being of similar size in contrast to those included in our interspecific analyses. When variation in size is reduced, behavioral variation and plastic changes in muscles among individuals within a species may become more powerful factors, causing discrepancies between *in vivo* bite force and estimated bite force. In

two species out of four studied here, we were able to get a good fit between modelled and real values. For *R. tanezumi*, this correlation is mostly due to size, but musculature still plays a significant role. For *M. cervicolor* the good fit of estimated values despite a limited variation in size probably reveals a very significant effect of muscle differences on bite force. In *R. exulans*, no correlation was found between *in vivo* bite force and estimated bite force, but when removing the effect of size, both values did correlate. It implies that size-independent muscle differences induce bite force differences in this species. This counterintuitive result might be due to the commensal niche occupied by this rat. Indeed, *R. exulans* has been frequently caught in basements, or around human infrastructures feeding on waste, rice stocks, or even farm animal food. These types of food may provide a very rich, yet rather soft diet, compared to that of wild animals. Such a diet may therefore allow normal or increased growth (due to the nutritional value of the food) while being functionally less demanding (due to its softness), furthermore very fine scale diet adaptation may be permitted by a great plasticity. Our results also show that one should exercise more caution when using biomechanical models for bite force at the intraspecific levels than at the interspecific level.

Populations of *M. pahari* and *M. caroli* from the lab are clearly differentiated from other species (including their wild conspecifics), with a much higher *in vivo* than estimated bite force. This could be due to an effect from laboratory rearing, as these lab mice show disproportionate muscle weights compared to their wild counterparts (Table 1), which may bias the bite force estimations. These mice may also be in generally better condition due to lowered threats (predation, parasites, and stress). Another explanation may be that the *in vivo* bite force used for these lab-reared specimens was not measured on the same specimens as the ones we dissected, but correspond to a mean value of the colony.

As expected, independent contrasts analyses showed strongly correlated evolution between size and bite force, independent of phylogeny. Furthermore, estimated bite force and *in vivo* bite force were still correlated independently of phylogeny and size, suggesting that skull morphology and muscular attributes also play a significant role in shaping performance. Based on Pagel's lambda values, it appears that size is not independent of phylogeny in our case. This nonindependence is probably due to the split between mice (smaller) and rats (bigger), which structures the size variation along the tree (Fig. 2). Furthermore, the scalings of musclular mass with size appeared to be different from the scalings of their independent contrasts, suggesting that phylogeny is also related to changes in the allometry of the muscles. Due to the strong correlation between size and bite force, the phylogenetic signal on size, and on the allometry of the muscles is likely the main factor explaining a potential effect of phylogeny on *in vivo* or estimated bite force when not correcting for the effect of size. As previously mentioned, the sole effect of size is not sufficient to fully explain the correlation between *in vivo* bite force and estimated bite force. Indeed, variation in the musculature was found to be correlated with bite force. However, most of this variation was also explained by the positive allometric relationships between muscles and size (Table 2). The remaining differences in muscles (i.e., nonallometric structural differences) between species did not correlate to size-independent differences in bite force, and followed a white noise (i.e. random) model of evolution. This may indicate that rodents can rapidly evolve their muscular organisation, or that it can be subject to important phenotypic plasticity. In any case, these changes do not appear directly linked to performance, which could suggest a case of many-to-one mapping, as found in other mammals (Young et al. 2007). Overall, size has a twofold effect on bite force: firstly via the phylogenetically driven size changes among species, whereby bigger animals have stronger bites; and secondly via the positively allometric differences in musculature, meaning that muscular mass (and PCSA) increases more than expected with size among species (Table 2). At a wider scale, when we compare the scaling of muscles in rodents with those of bats (Herrel et al. 2008a), it appears that muscle masses scale much more positively in the former. This may bring support to the hypothesis that bats have important muscle mass limitations due to flight. Interestingly, the slope of bite force against size is much smaller in bats (1.71) than in rodents (2.01 for *in vivo* bite force and 2.84 for estimated bite force; Fig. 4), which illustrates the twofold effect of size on bite force in our group of interest.

When accounting for the influence of size, the remaining phylogenetic effect on bite force was limited and the evolution of the bite force appeared to be random. Similarly, size-independent muscular variation was small and apparently random among our species. These elements are coherent with the hypothesis that skull structure and mechanics are quite stable in myomorphous rodents, or at least in murids. Indeed the randomness of size-independent variation and its limited scale suggest very subtle adaptive changes, and/or a more important role of plasticity. In other terms, the overall skull structure and function was conserved during the evolutionary history of our sample of the Muridae and skull evolution was mainly related to that of size, but morphological changes still appear to have happened, although they may not have produced large differences in performance. This could indicate that most murid rodents have a functional output that enables them to use a wide range of resources without requiring major morphological changes, and/or that architectural constraints of the skull limit major muscular changes. Other myomorphous rodent groups may show similar high performance through their convergence in skull morphotype, although we did not include any in this study. We also showed that skull size alone drives most of the functional changes observed in our species. Since size- and allometry-independent variation in musculature does not appear to be related to size-independent bite force differences, our results might also be explained by the fact that different anatomies may produce similar functional outputs (Bock 1959, Schmidt-Kittler 1997, Alfaro et al. 2005, Young et al. 2007).

Even if our results hold true for bite force, other functionally significant elements of performance may also vary with musculature, such as bite force at different gape angles or angular speed of jaw closure (e.g., Satoh and Iwaku 2006, Santana and Portugal 2016). Other available models for bite force estimation, such as those including the 3D skull morphology may also improve the precision of estimations (e.g., Davis et al. 2010). Indeed,

the 2D representations of the muscular attachments and line of actions used here may be a source of error in the modeled bite force. Another caveat is that we only tested muscular variation in terms of mass, fiber length, and PCSA against bite force. We did not test for an effect of bone morphology modifications on muscle organization. Indeed, size- and phylogeny-independent variation in mass, fiber length, and PCSA is reduced, but functional adaptation may for example be brought via changes in lever arms rather than in muscle themselves.

Our conclusions may not apply to all myomorphous rodents since our dataset was strictly restricted to a limited number of murine species. Furthermore, our dataset lacked extreme specialists. While mice and rats are often regarded as best representatives of the myomorphous morphotype, it is clear that other myomorphous rodents (e.g., Cricetidae and Gliridae) depart from the skull variation seen in murines. Owing to the predictive power of our biomechanical models, it would be now particularly interesting to ascertain the biomechanical implications of the zygomasseteric arrangement in glirids that convergently evolved a pseudomyomorphous type of skull (*sensu* Vianey-Liaud 1989, but see also Hautier et al. 2008).

ACKNOWLEDGEMENTS

The authors would like to thank Serge Morand and other members of the Ceropath and Biodiv-healthSEA projects who helped organize and participated in the field work. They are also very grateful to Frederic Veyrunes and Jean-Jacques Duqesne who gave some specimens and allowed us to measure bite forces in their lab colonies. Pierre-Henri Fabre's help with the phylogeny was invaluable. Finally, they would like to Adam Hartstone-Rose for the invitation to participate in this issue, and S. Santana and two anonymous reviewers for their helpful and constructive comments. Parts of the experiments were performed using the μ-CT facilities of the MRI platform and of the LabEx CeMEB. This publication is a contribution of the Institut des Sciences de l'Evolution de Montpellier (UMR 5554 – UM2 + CNRS + IRD) No. ISEM 2017-280

LITERATURE CITED

Aguirre LF, Herrel A, van Damme R, Matthysen E. 2002. Ecomorphological analysis of trophic niche partitioning in a tropical savannah bat community. Proc R Soc Lond B 269:1271–1278.

Aguirre LF, Herrel A, van Damme R, Matthysen E. 2003. The implications of food hardness for diet in bats. Funct Ecol 17:201–212.

Alfaro ME, Bolnick DI, Wainwright PC. 2005. Evolutionary consequences of many-to-one mapping of jaw morphology to mechanics in labrid fishes. Am Nat 165:E140–E154.

Aplin KP, Suzuki H, Chinen AA, Chesser RT, Ten Have J, Donnellan SC, Austin J, Frost A, Gonzalez JP, Herbreteau V, et al. 2011. Multiple geographic origins of commensalism and complex dispersal history of black rats. PLoS ONE 6:e26357.

Baverstock H, Jeffery NS, Cobb SN. 2013. The morphology of the mouse masticatory musculature. J Anat 223:46–60.

Becerra F, Echeverria A, Vassallo AI, Casinos A. 2011. Bite force and jaw biomechanics in the subterranean rodent Talas tuco-tuco (*Ctenomys talarum*) (Caviomorpha: Octodontoidea). Can J Zool 89:334–342.

Berry RJ, Jakobson ME. 1975. Adaptation and adaptability in wild-living House mice (*Mus musculus*). J Zool 176:391–402.

Bock WJ. 1959. Preadaptation and multiple evolutionary pathways. Evolution 13:194–211.

Brandt JF. 1855. Untersuchungen über die craniologischen Entwicklungsstufen und Classification der Nage der Jetzwelt. Mémoires de l'Academie Imperiale des Sciences de St Pétersbourg Série 6 9:1–365.

Corbalàn V. 2006. Microhabitat selection by murid rodents in the Monte desert of Argentina. J Arid Environ 65:102–110.

Cornette R, Baylac M, Souter T, Herrel A. 2013. Does shape covariation between the skull and the mandible have functional consequences? A 3D approach for a 3D problem. J Anat 223:329–336.

Cox PG, Fagan MJ, Rayfield EJ, Jeffery NS. 2011. Finite element modelling of squirrel, guinea pig and rat skulls: Using geometric morphometrics to assess sensitivity. J Anat 219:696–709.

Cox PG, Rayfield EJ, Fagan MJ, Herrel A, Pataky TC, Jeffery NS. 2012. Functional evolution of the feeding system in rodents. PLoS ONE 7:e36299.

Davis JL, Santana SE, Dumont ER, Grosse IR. 2010. Predicting bite force in mammals: Two dimensional versus three dimensional lever models. J Exp Biol 213:1844–1851.

Druzinsky RE. 2010. Functional anatomy of incisal biting in *Aplodontia rufa* and sciuromorph rodents – part 2: Sciuromorphy is efficacious for production of force at the incisors. Cells Tissues Organs 192:50–63.

Fabre P-H, Pagès M, Musser GG, Fitriana YS, Fjeldså J, Jennings A, Jønsson KA, Kennedy J, Michaux J, Semiadi G, et al. 2013. A new genus of rodent from Wallacea (Rodentia: Muridae: Murinae: Rattini), and its implication for biogeography and Indo-Pacific Rattini systematics. Zool J Linn Soc 169:408–447.

Felsenstein J. 1985. Phylogenies and the comparative method. Am Nat 125:1–15.

Freeman PW, Lemen CA. 2008a. A simple morphological predictor of bite force in rodents. J Zool 275:418–422.

Freeman PW, Lemen CA. 2008b. Measuring bite force in small mammals with a piezo-resistive sensor. J Mammal 89:513–517.

Harmon LJ, Weir JT, Brock CD, Glor RE, Challenger W. 2008. GEIGER: Investigating evolutionary radiations. Bioinformatics 24:129–131.

Hautier L, Cox P, Lebrun R. 2015. Grades and clades among rodents: The promise of geometric morphometrics. In: Cox P & Hautier L, editors. Evolution of the rodents: Advances in phylogeny, functional morphology and development. Cambridge: Cambridge University Press. p 277–299.

Hautier L, Michaux J, Marivaux L, Vianey-Liaud M. 2008. The evolution of the zygomasseteric construction in Rodentia, as revealed by a geometric morphometric analysis of the mandible of *Graphiurus* (Rodentia, Gliridae). Zool J Linn Soc 154:807–821.

Herrel A, Aerts P, De Vree F. 1998a. Ecomorphology of the lizard feeding apparatus: A modelling approach. Neth J Zool 48:1–25.

Herrel A, Aerts P, De Vree F. 1998b. Static biting in lizards: Functional morphology of the temporalis ligaments. J Zool 244:135–143.

Herrel A, Spithoven L, Van Damme R, De Vree F. 1999. Sexual dimorphism of head size in *Gallotia galloti*: Testing the niche divergence hypothesis by functional analyses. Funct Ecol 13:289–297.

Herrel A, De Smet A, Aguirre LF, Aerts P. 2008a. Morphological and mechanical determinants of bite force in bats: Do muscles matter?. J Exp Biol 211:86–91.

Herrel A, Huyghe K, Vanhooydonck B, Backeljau T, Breugelmans K, Grbac I, van Damme R, Irschick DJ. 2008b. Rapid large-scale evolutionary divergence in morphology and performance associated with exploitation of a different dietary resource. PNAS 105:4792–4795.

Herrel A, Moore JA, Bredeweg EM, Nelson NJ. 2010. Sexual dimorphism, body size, bite force and male mating success in tuatara. Biol J Linn Soc 100:287–292.

Herrel A, Podos J, Huber SK, Hendry AP. 2005. Bite performance and morphology in a population of Darwin's finches: Implications for the evolution of beak shape. Funct Ecol 19:43–48.

Herzog W. (1994). Muscle. In Biomechanics of the Musculoskeletal System (ed. B. M. Nigg and W. Herzog), pp. 154–187. Chichester: John Wiley.

Le Roux V, J-L C, Y F, P V. 2002. Diet of the house mouse (*Mus musculus*) on Guillou Island, Kerguelen archipelago, Subantarctic. Polar Biol 25:49–57.

Maestri R, Patterson BD, Fornel R, Monteiro LR, De Freitas TRO. 2016. Diet, bite force and skull morphology in the generalist rodent morphotype. J Evol Biol 29:2191–2204.

Michaux J, Chevret P, Renaud S. 2007. Morphological diversity of Old World rats and mice (Rodentia, Muridae) mandible in relation with phylogeny and adaptation. J Zool Syst Evol Res 45:263–279.

Navarrete SA, Castilla JC. 1993. Predation by Norway rats in the intertidal zone of central Chile. Mar Ecol Prog Ser 92:187–199.

Nies M, Ro JY. (2004). Bite force measurement in awake rats. Brain research protocols, 12:180–185.

R Core Team. 2016. R: A language and environment for statistical computing. Vienna, Austria: R Foundation for Statistical Computing. Url https://www.R-project.org/.

Rowe KC, Aplin KP, Baverstock PR, Moritz C. 2011. Recent and rapid speciation with limited morphological disparity in the genus *Rattus*. Syst Biol 60:188–203.

Samuels JX. 2009. Cranial morphology and dietary habits of rodents. Zool J Linn Soc 156:864–888.

Santana SE, Dumont ER. 2009. Connecting behaviour and performance: The evolution of biting behaviour and bite performance in bats. J Evol Biol 22:2131–2145.

Santana SE, Dumont ER, Davis JL. 2010. Mechanics of bite force production and its relationship to diet in bats. Funct Ecol 24:776–784.

Santana SE, Portugal S. 2016. Quantifying the effect of gape and morphology on bite force: Biomechanical modelling and *in vivo* measurements in bats. Funct Ecol 30:557–565.

Satoh K. 1997. Comparative functional morphology of mandibular forward movement during mastication of two Murid rodents, *Apodemus speciosus* (Murinae) and *Clethrionomys rufocanus* (Arvicolinae). J Morphol 231:131–142.

Satoh K, Iwaku F. 2006. Jaw muscle functional anatomy in northern grasshopper mouse, *Onychomys leucogaster*, a carnivorous murid. J Morphol 267:987–999.

Satoh K, Iwaku F. 2008. Masticatory muscle architecture in a murine murid, *Rattus rattus*, and its functional significance. Mammal Study 33:35–42.

Schmidt-Kittler N. 1997. Non-selective emergence of patterns and gradual change in macroevolution. Courier Forschungsinstitut Senckenberg 201:393–408.

Siahsarvie R, Auffray J-C, Darvish J, Rajabi-Maham A, Yu H-T, Agret S, Bonhomme F, Claude J. 2012. Patterns of morphological evolution in the mandible of the house mouse *Mus musculus* (Rodentia: Muridae). Biol J Linn Soc 105:635–647.

Suzuki H, Shimada T, Terashima M, Tsuchiya K, Aplin K. 2004. Temporal, spatial, and ecological modes of evolution of Eurasian *Mus* based on mitochondrial and nuclear gene sequences. Mol Phylogenet Evol 33:626–646.

Tullberg T. 1899. Über das System der Nagetiere. Eine phylogenetische studie. Nova Acta Regiae Societatis Scientiarium Upsaliensis 18:1–514.

Van Daele PAAG, Herrel A, Adriaens D. 2009. Biting performance in teeth-digging African mole-rats (*Fukomys*, Bathyergidae, Rodentia). Physiol Biochem Zool 82:40–50.

Verwaijen D, van Damme R, Herrel A. 2002. Relationships between head size, bite force, prey handling efficiency and diet in two sympatric lacertid lizards. Funct Ecol 16:842–850.

Veyrunes F, Britton-Davidian J, Robinson TJ, Calvet E, Denys C, Chevret P. 2005. Molecular phylogeny of the African pygmy mice, subgenus *Nannomys* (Rodentia, Murinae, *Mus*): Implications for chromosomal evolution. Mol Phylogenet Evol 36:358–369.

Vianey-Liaud M. 1989. Parallelism among Gliridae (Rodentia): The genus *Gliravus* Stehlin and Schaub. Hist Biol 2:213–226.

Waterhouse GR. 1839. Observations on the Rodentia with a view to point out groups as indicated by the structure of the crania in this order of mammals. Magaz Nat Hist 3:90–96. 184–188, 274–279, 593–600.

Young RL, Haselkorm TS, Badyaev AV. 2007. Functional equivalence of morphologies.